scientific reports

Check for updates

OPEN

Experimental ex vivo characterization of the biomechanical effects of laminectomy and posterior fixation of the lumbo-sacral spine

Sara Montanari[1], Giovanni Barbanti Bròdano[2], Elena Serchi[3], Rita Stagni[4], Alessandro Gasbarrini[2], Alfredo Conti[3,5] & Luca Cristofolini[1]✉

Laminectomy and posterior fixation are well-established surgical techniques to decompress nervous structures in case of lumbar spinal stenosis. While laminectomy is suspected to increase the instability of the spine, posterior fixation is associated with some complications such as adjacent segment degeneration. This study aimed to investigate how laminectomy and posterior fixation alter the biomechanics of the lumbar spine in terms of range of motion (ROM) and strains on the intervertebral discs. Twelve L2-S1 cadaveric spines were mechanically tested in flexion, extension, and lateral bending in the intact condition, after two-level laminectomy and after L4-S1 posterior fixation. The ROM of the spine segment was measured in each spine condition, and each loading configuration. The strain distribution on the surface of all the intervertebral discs was measured with Digital Image Correlation. Laminectomy significantly increased the ROM in flexion ($p = 0.028$) and lateral bending ($p = 0.035$). Posterior fixation decreased the ROM in all the loading configurations. Laminectomy did not significantly modify the strain distribution in the discs. Posterior fixation significantly increased the principal tensile and compressive strains in the disc adjacent the fixation both in flexion and in lateral bending. These findings can elucidate one of the clinical causes of the adjacent segment degeneration onset.

Lumbar spinal stenosis is defined as the compression of the neural elements due to the narrowing of the space within the spinal canal, the nerve canals, or the neural foramina[1]. This disorder may occur due to congenital or degenerative factors, or a combination of both. Spinal stenosis predominantly afflicts elderly people[1–4], being the main cause of lumbar spine surgery in adults over 65 years old[5]. Laminectomy (Fig. 1) is the common procedure to decompress the central canal and the lateral recesses to relief common stenotic symptoms, such as neurogenic claudication and radiculopathy. Laminectomy is associated with relatively high satisfaction and improved long-term outcome[6,7]. However, laminectomy can compromise the normal biomechanics of the spinal segment, leading to iatrogenic instability and postoperative iatrogenic spondylolisthesis[3,8]. These complications significantly impact the clinical outcomes and increase the risk of revision surgery[9]. In order to avoid these complications, posterior fixation (Fig. 1) is frequently associated with laminectomy. Unfortunately, adding posterior instrumentation (pedicle screws and rods) was associated with some complications, like more bleeding, longer hospitalization[10], increased incidence of hardware-related complications and of adjacent segment degeneration. The adjacent segment degeneration is defined as the symptomatic deterioration of the intervertebral disc adjacent to a previous fusion and is seen predominantly at the adjacent cranial levels.

Recent clinical studies did not find consistent clinical benefits in patients subjected to decompression with fusion rather than in patients subjected to decompression surgery alone[10–13]. Different outcomes may be due to different patient inclusion criteria, different technique to perform decompression surgery, presence or absence

[1]Department of Industrial Engineering, School of Engineering and Architecture, Alma Mater Studiorum – University of Bologna, Via Umberto Terracini 24-28, Bologna 40131, Italy. [2]Spine Surgery Department, IRCCS Rizzoli Orthopaedic Institute, Bologna, Italy. [3]Neurosurgery Unit, IRCCS Istituto delle Scienze Neurologiche di Bologna, Bologna, Italy. [4]Department of Electrical, Electronic and Information Engineering "Guglielmo Marconi", Alma Mater Studiorum – University of Bologna, Bologna, Italy. [5]Department of Biomedical and Neuromotor Sciences (DIBINEM), Alma Mater Studiorum – University of Bologna, Bologna, Italy. ✉email: luca.cristofolini@unibo.it

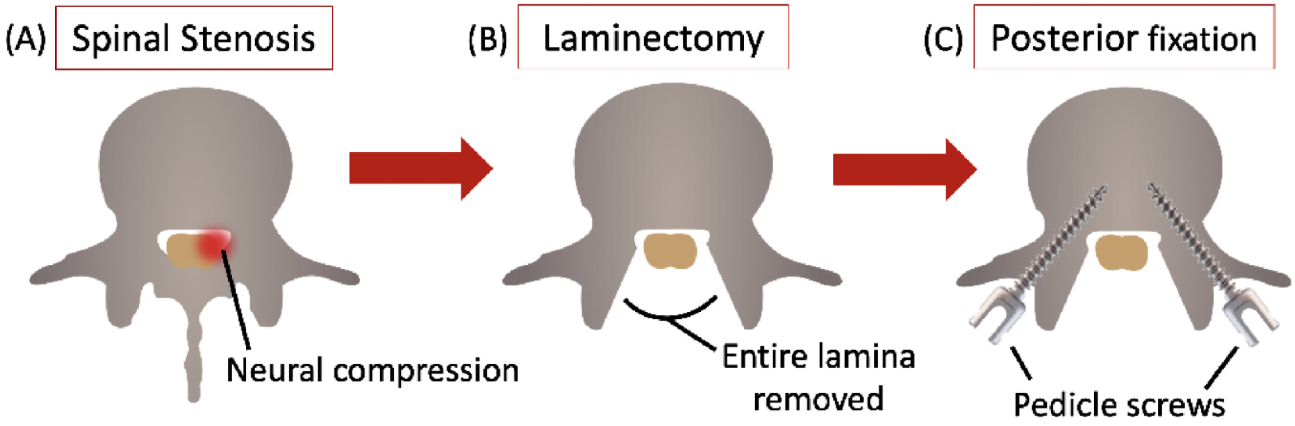

Fig. 1. Schematic representation of the clinical problem, the lumbar spinal stenosis (**A**), and of the two different surgical procedures that can be performed: removal of the lamina (laminectomy) (**B**), and laminectomy stabilized with posterior fixation with pedicle screws and rods (**C**). Figure published on Figshare repository (https://doi.org/10.6084/m9.figshare.25823851).

of spondylolisthesis or other degenerative diseases that could affect the final outcome. Therefore, the debate in the literature is still open.

After fixation, the mobility of the segments decreases, resulting in a compensatory effect which involves an increase in the motion of the adjacent segments, causing stress concentration and accelerated degeneration[14]. The adjacent segment degeneration after spine posterior fixation can occur both in the cranial and caudal segments. Clinically, the cranial segments are more likely to be subjected to degeneration with an higher incidence than caudal segments[15,16]. Despite this, a recent study demonstrated that junctional pathology has an high incidence also in the caudal extremity of the instrumented fixation[17].One of the reasons why the degeneration of the adjacent segment may occur could be the abnormal strains concentration on the adjacent intervertebral discs. Ma et al., 2014[18] evaluated experimentally the strain distribution on the facet joints of the fixated spine segments. Bisschop et al., 2015[19] assessed the segmental stiffness after laminectomy and fixation on cadaver spine segments. However, to the Authors' best knowledge, no study in the literature analysed how the strain distribution in the intervertebral discs is affected by either laminectomy or posterior fixation.

In addition, stenosis at multiple levels has a high incidence compared to the incidence of the strictly segmental stenosis[1]. L3-L4 and L4-L5 are reported as the most affected segments[1]. Moreover, the risk of postoperative complications and listhesis increases with the increasing number of decompressed levels[20,21]. Despite that, in the literature most studies focused on single-level laminectomy and posterior fixation.

The purpose of this ex vivo study was to investigate, on longer spine segments than commonly used in previous studies, if two-level laminectomy alone, or completed by a lumbo-sacral posterior fixation could have a worsening biomechanical effect on the lumbar spine. In particular, first, this study aimed to assess the changes of the mobility of the lumbar spine after two-level laminectomy and after fixation. In addition, we aimed to investigate if laminectomy and posterior fixation affect the strain distribution on the lumbar intervertebral discs, in a way that could aggravate the degeneration of the discs between the treated levels or in the adjacent ones.

Methods

L4-L5 are the most frequent levels where the lumbar stenosis occurs. In order to study the effect of the decompression applied to these levels, and the fixation on the L4-S1 levels, twelve L2-S1 segments were extracted and prepared for testing so as to include also the cranial and caudal levels, and an additional vertebra for load application in the testing machine. A two-level laminectomy at L4 and L5 vertebrae, and L4-S1 posterior fixation with pedicle screws and rods were sequentially performed (Fig. 1) by an expert neurosurgeon and by an expert spine surgeon, respectively. All the specimens were mechanically tested in the intact condition, after the laminectomy and after the posterior fixation, under the same loading configurations: flexion, extension, left and right lateral bending. Digital Image Correlation (DIC) was used to measure the spatial displacements, and the strain distribution on the intervertebral discs.

Ethics

This study was approved by the Bioethics Committee of University of Bologna (Prot. n. 113043 of 10 May 2021). The work was performed in line with the principles of the Declaration of Helsinki. All the spine cadavers were obtained from an ethically approved donation program (Anatomy Gift Registry, AGR), which obtained the informed consent from all the subjects.

Selection and imaging of the specimens

Twelve L2-S1 spine segments were extracted and prepared from twelve fresh frozen human cadavers (5 females, 7 males, median age 74 years, median BMI 30 kg/m^2) (Table 1). All specimens were frozen at −28 °C and sealed in a double plastic bag until prepared and tested.

Specimen	Sex	Age (years)	BMI (kg/m^2)	Cause of death
#1	M	70	32	Myocardial infarction
#2	M	79	25	Stroke
#3	F	75	40	Arteriosclerotic cardiovascular
#4	F	82	23	Cardiac arrest
#5	M	76	22	Arteriosclerotic cardiovascular disease
#6	M	74	27	Anoxic brain injury
#7	F	56	48	Septic shock
#8	F	75	51	Sepsis
#9	M	62	17	Blunt force trauma
#10	M	72	26	End stage liver disease
#11	F	62	43	Glioblastoma
#12	M	73	36	Aspiration pneumonia
Median	-	74	30	-
IQR	-	7	16	-

Table 1. Specimens' data. The first columns summarize the donors' information. The cause of death is detailed in the last column. Median and interquartile range (IQR) are reported for age and BMI.

The spine specimens were scanned twice with computer tomography (CT, G.E. Revolution HD 1700, current: 80 mA, voltage: 120 kV, slice thickness: 0.625 mm). CT scans of the whole spines were initially acquired to check the status of each spine in terms of disc degeneration, osteophytes, ligament calcifications, and bone fusion, and to confirm the absence of previous fractures, surgeries, tumours or metastases.

After preparation of the specimens (see below), further CT images of each L2-S1 spine segment were taken (with the same parameters, and including a densitometric calibration with a European Spine Phantom, ESP) to specifically define in which cases osteophytes should be removed, and to measure the dimensions of the vertebrae.

Specimens preparation

Before starting the preparation of the specimens, the whole spines were thawed at room temperature. The L2-S1 segment was extracted from each spine. Particular attention was given to preserve intact the intervertebral discs, the facet joint capsule and the ligamentous structures to be sure to preserve the natural kinematics of the lumbar spine[22]. Conversely, skin, fat and muscles were carefully removed.

Then, the upper half of the most cranial vertebra (L2) and the lower half of the most caudal vertebra (S1) were embedded in acrylic resin (Technovit 4071, Heraeus Kulzer, Wehrheim, Germany) to mount the specimens in the testing machine. Additionally, to ensure that all the specimens were mounted reproducibly[23] and that mechanical loading was applied properly to all the specimens, each spine segment was aligned with the L4 vertebra horizontal in both the sagittal and the transversal planes, by means of a six-degree-of-freedom clamp and following a reproducible and suitable published procedure[24]. Finally, based on both the CT scans and visual inspection, osteophytes were assessed by a surgeon and removed in case of bridging or if they obstructed the kinematics (details are provided in the Supplementary Information, Table S1).

Surgical procedures

Laminectomy

After being tested in the intact condition in all the loading configurations (see below), a two-level laminectomy was performed on the twelve specimens at the L4 and L5 vertebrae (Fig. 2) by an expert neurosurgeon, who replicated the same surgery which is performed on patients suffering from lumbar spinal stenosis. After the identification of the L4 and L5 vertebrae and of related spinous process, the supraspinous and interspinous ligaments between L3 and L4 and between L5 and S1 were cut with a scalpel. The L4 and L5 spinous processes were detached (exposing the ligamentum flavum and the epidural fat). From the junction between the lamina and the removed spinous process, to lateral side until the junction with both the facet joints, the L4 and L5 laminae were removed by means of Kerrison rongeurs. This allowed to expose the ligamentum flavum and the epidural fat in order to free the canal without damaging the dural sac.

Surgical procedures

Posterior fixation

After being tested in the laminectomy condition in all the loading configurations, a posterior fixation was performed on the L4-S1 levels on all the specimens by an expert spine surgeon (Fig. 2), using a commercial kit and its proprietary instrumentation, and following the same procedure that is normally applied on patients suffering from lumbar spinal stenosis. First, the spine surgeon identified the pedicles of the L4, L5, and S1 vertebrae and inserted the polyaxial pedicle screws ($\Phi = 6$ mm, $L = 40$ mm, Saxxo system, MediNext), first in one side and then in the other. Finally, after shaping the titanium rods (Saxxo system, MediNext) so as to recover the desired physiological curvature of the lumbar segment, the surgeon connected the rods with the screws and tightened the respective nuts.

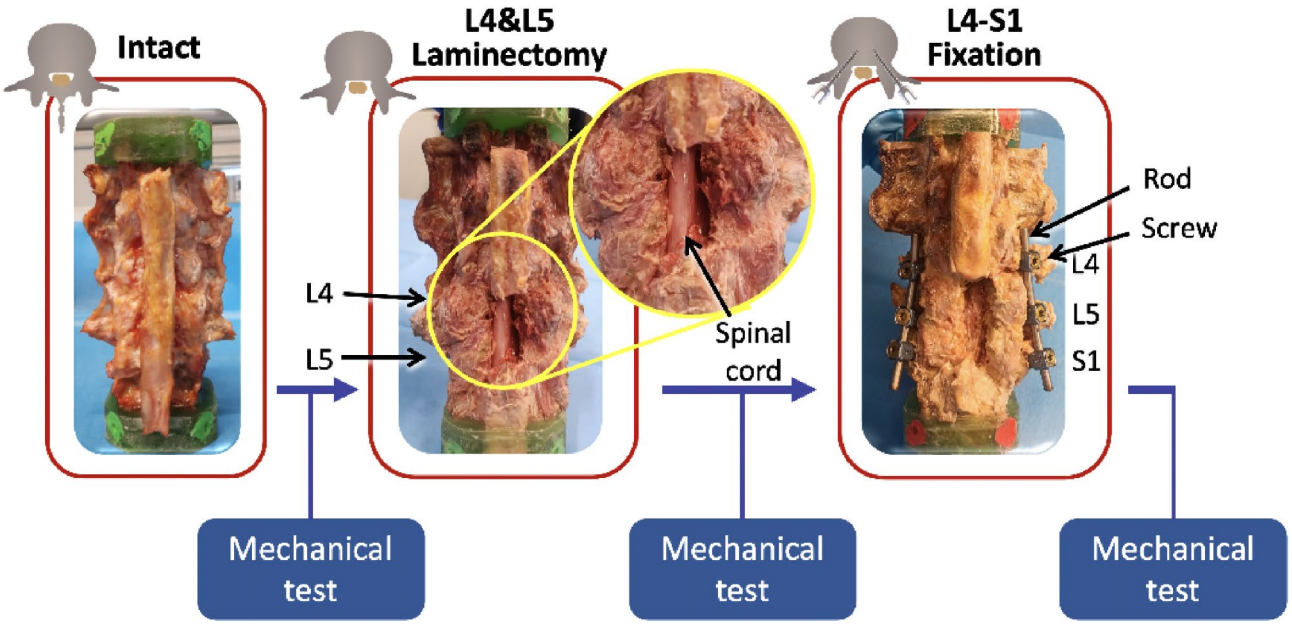

Fig. 2. Workflow of the study. Twelve L2-S1 human spine segments were prepared and tested in the intact condition. Then, a two-level laminectomy was performed at the L4 and L5 levels by an expert neurosurgeon. Finally, an expert spine surgeon performed a posterior fixation on L4-S1 levels with pedicle screws and rods. Each specimen was mechanically tested under the same loading configurations in each condition. Figure published on Figshare (https://doi.org/10.6084/m9.figshare.25823881).

Mechanical tests

Each specimen was mechanically tested in flexion, extension and both left and right lateral bending, under the same testing parameters: (i) in the intact condition, (ii) after the L4 and L5 laminectomy, and (iii) after the L4-S1 posterior fixation. Each test was performed in displacement control by means of a servo-hydraulic testing machine (Instron 8500 controller, Instron, UK) equipped with a 10 kN load cell. During each mechanical test, a combination of force and bending was applied in order to reach the target moment of 2.5 Nm. In order to avoid the risk of damaging the specimen during repeated testing before and after surgery, a relatively low bending moment of 2.5 Nm was intentionally chosen. The cranial extremity of the specimen (L2 vertebra, embedded in the acrylic pot) was rigidly attached to the actuator of the testing machine by means of a metallic plate (Fig. 3). Conversely, the caudal extremity of the specimen was linked to a spherical joint moving along a low friction rail. In this way, each specimen was free to follow its natural relative motion, and rotations and translations in the horizontal plane were allowed. In the middle, a micrometric adjustable bidirectional slide was placed to apply the force with the desired offset with respect to the centre of the L4 vertebra, in order to reach the target moment. Applying an anterior, posterior or lateral offset allowed to generate flexion, extension or lateral bending respectively. The offset was computed on the specific anatomy of each specimen, from the CT images, as a percentage of the length and width of the L4 vertebra (Supplementary Information, Table S1). In particular, an offset of 30% of the antero-posterior length of the vertebra was applied in case of flexion, and an offset of 100% of the antero-posterior length was decided in extension, as the lumbar spine is more flexible in flexion compared to extension. However, in three specimens the lordotic curvature was nearly absent, the offset was increased to 150% of the antero-posterior length of L4. Lastly, an offset of the 50% of the right-left width of the L4 vertebra was applied for both the left and right lateral bending.

An initial preload of 20 N was applied to stabilize the specimen. A preconditioning, consisting of 20 sinusoidal cycles at 0.5 Hz, was performed before the test of each loading configuration (Fig. 3). Subsequently, each test repetition consisted of six trapezoidal cycles (Fig. 3), where the loading ramp lasted 1.0 s, the maximum load was held constant for 0.3 s, and then the specimen was unloaded in 0.5 s[25]. The first three cycles of each repetition were sufficient for minimizing the viscoelastic response[23,26], the subsequent cycles being nearly identical in terms of loads and displacements[25]. So, the data from the last cycle were extracted and analysed. Each test was repeated five times to have enough data in case of any problems during the mechanical tests. The data from the last three repetitions were used to assess the repeatability of the test method and extracted for analysis and averaged.

All the tests were performed at room temperature, and the specimens were wrapped in wet paper moistened with saline to keep hydration of tissues while the test rig was adjusted for the different loading configurations[23].

Data acquisition with the digital image correlation

Digital image correlation (DIC) is a full-field, contactless optical method for measuring surface displacement and strain of a loaded structure[27,28]. This technique computes the displacements of each point on the surface of the specimen throughout the experiment. The strain field is then obtained by derivation. Validated and certified algorithms for computing displacements and strains are commercially available. In this study, a state-

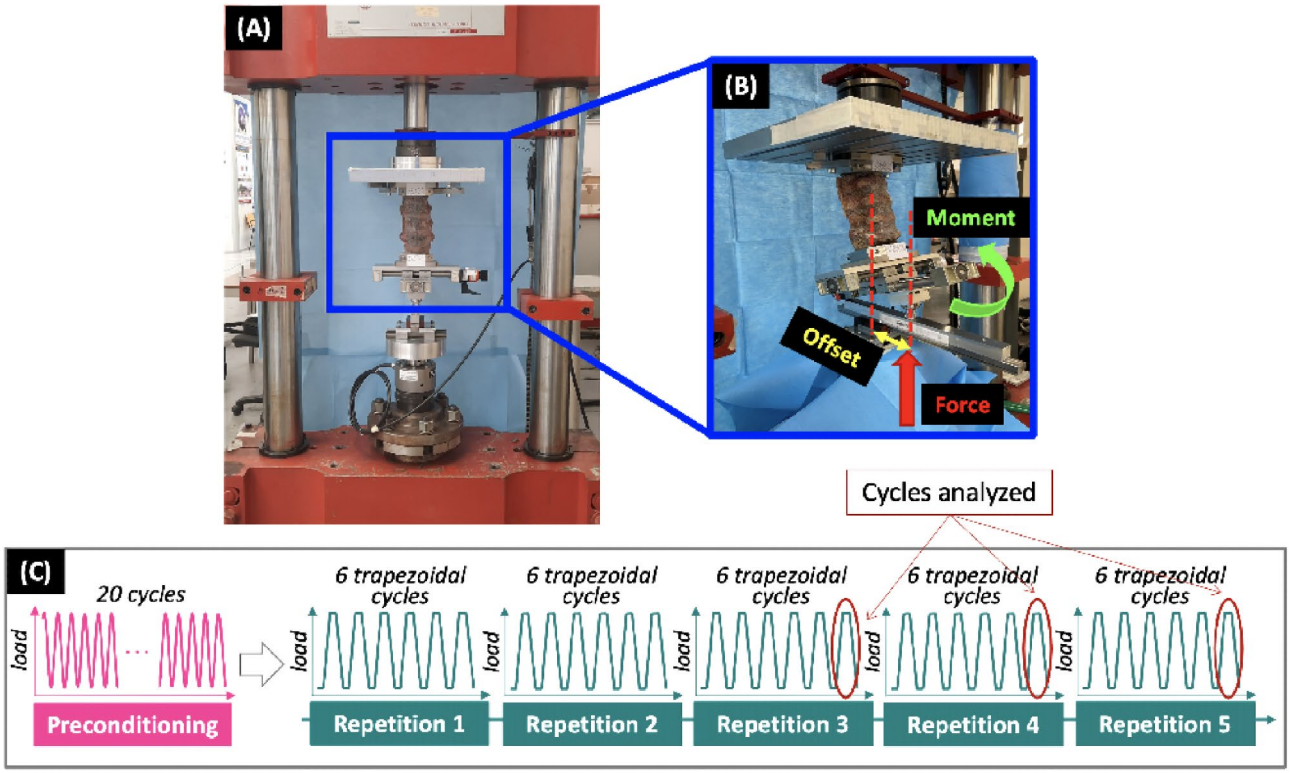

Fig. 3. Set-up of the mechanical test. (**A**) Overview of the specimen mounted in the testing machine, and (**B**) detail how the micrometric adjustable bidirectional slide allowed to apply the desired offset. The experimental testing sequence (**C**), which was replicated in all the different loading configurations, included a pre-conditioning and five repetitions of 6-cycle test. The red ellipses highlight the last cycle of each repetition, where the data were extracted and analysed. Figure published on Figshare (https://doi.org/10.6084/m9.figshare.25823887).

of-the-art Digital Image Correlation system (Aramis Adjustable 12 M, GOM, Braunschweig, Germany) with the proprietary algorithm, was used during the mechanical tests to measure the spatial displacements and the strain distributions[29] on the surface of each specimen. Both the anterior and lateral side (including both the vertebrae and the intervertebral discs) were acquired by the DIC system equipped with four cameras. The four cameras had a resolution of 12Mpixel (4096×3000) and were equipped with metrology-quality lenses Titanar B 75 (f 4.5), and a light system with 4 LEDs light with 10° light cone (Fig. 4). Each pair of cameras provides stereoscopic vision, and the calibration process allows to quantify the errors in all the directions. The two pairs of cameras are configured and calibrated to measure out-of-plane displacement components as well. The angles and parameters for which the system is certified are such as to ensure that similar errors apply to the in-plane and out-of-plane components.

The system was calibrated with a proprietary calibration target (Type CP40/200/101296t GOM, Aramis, Braunschweig, Germany) before each test. During the calibration process, the proprietary calibration target was placed at different positions and angles in the measuring volume in order to calculate the coefficients for the particular optics configuration adopted, and simultaneously assess the calibration residuals. Low values of the calibration residuals are an indicator of high accuracy and precision, and small in-plane and out-of-plane errors.

Images during the relevant loading cycles were acquired at 25 frames per second.

To allow the DIC system to measure the strain distribution during the mechanical tests, a white pattern (Fig. 4) was sprayed on the antero-lateral surface of each specimen using a water-based acrylic paint (Q250201 Bianco Opaco, Chreon, Italy). In order to achieve reliable correlation results, the speckle pattern should have a random distribution, a high contrast, and a white-to-black contrast ratio with the background close to 50:50. The size of the speckle dots should be 2–3 times the pixel dimension of the acquired image[27]. Therefore, the air pressure, airflow, dilution, and distance from the specimen were optimized to achieve the desired size of the speckle dots, following a published procedure[27,30]. In particular, the speckle pattern was prepared at room temperature with the following parameters: airbrush pressure of one bar, airflow with three turns of the screw in the airbrush, 20 ml of white paint diluted with 8 ml of water, and the paint was sprayed at the distance of 500 mm from each specimen[31].

Assessment of the measurement uncertainties

In order to assess the intrinsic uncertainties of the DIC measurements, a zero-strain analysis was performed on twoconsecutive unloaded images of each specimen[29]. If no loads are applied, no displacements and strain should

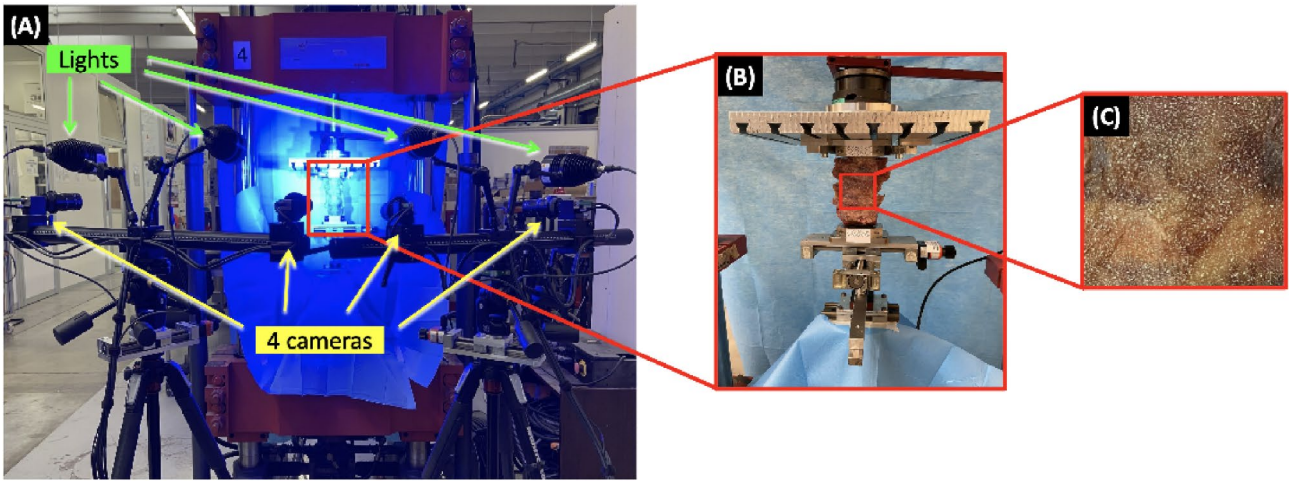

Fig. 4. Overview of the experimental setup with the four cameras of the Digital Image Correlation system (**A**), framing the specimen mounted in the testing machine (**B**). The zoomed detail of the specimen surface shows the white random speckle pattern sprayed on all the surface of the vertebrae and of the intervertebral discs (**C**). Figure published on Figshare (https://doi.org/10.6084/m9.figshare.25823893).

be theoretically measured. So, any value of displacement and strain different from zero should be accounted as measurement error. The systematic and random errors in this zero-strain configuration were quantified as indicatorsof the systematic and random errors affecting the DIC-measureddisplacements and strains. In order to choose the optimal DIC correlation parameters, a detailed analysis of the variation of the precision (quantified by the random error) of the strain measurements at different facet sizes, grid spacing, and resolution was performed (Supplementary Information, Fig. S2). In general, higher random errors are found with low values of the facet size and grid spacing. Conversely, large values of facet size and grid spacing reduce the spatial resolution. A facet size of 34 pixels, a grid spacing of 11 pixels with a spatial medial filter of the 5th order and a temporal average filter of the 2nd order was chosen as the optimal parameters after testing different combinations of facet size, grid spacing and filtering. This corresponded to a spatial resolution of ≈ 6 mm.

Data analysis

Data of the last loading ramp of the last cycle were analysed. Data from the last three repetitions were extracted and averaged for each spine condition and each loading configuration. In order to assess the repeatability of the repetitions in each loading configuration, the coefficient of variation was computed for each parameter as the ratio between the standard deviation and the average of the last three repetitions.

The range of motion (ROM) of the entire L2-S1 spine segment was computed to assess the variations in the mobility of the lumbar spine at the stage where the target moment of 2.5 Nm was reached (Fig. 5). In particular, ROM was measured as the relative rotation of the sacrum with respect to the L2 vertebra in the sagittal plane for flexion an extension, and in the coronal plane for both left and right lateral bending.

The maximum (tensile, ε1) and minimum (compressive, ε2) principal natural (true) strains were measured on the entire anterior and lateral surface of each specimen using the DIC dedicated software (Aramis Professional 2019, GOM) to assess the changes on the strain distribution in the intervertebral discs.

To assess if laminectomy alone, or with the addition of posterior fixation, creates a stress concentration at the treated levels or at the adjacent levels, an analysis of the largest and the mean values of both the tensile and compressive strain was performed on the regions of all the intervertebral discs. Specifically, to exclude local peaks due to measurement artifacts, the 95th (or 5th) percentiles were used as "largest" tensile (or compressive) values. In order to compare the strain at the comparable loading configuration of each condition, the strains were analysed at the stage where the intact and the laminectomy conditions reached the same rotation of the posterior fixation (Fig. 5).

To reduce the effect of the inter-specimen variability, the data in the laminectomy and in the fixation condition were normalized with respect to the intact condition of the respective specimen, for each loading configuration.

Statistical analysis

A statistical analysis was performed in order to assess the differences between the intact condition, the laminectomy alone, and the posterior fixation. The range of motion was analysed separately for each loading configuration. The largest and mean tensile strains and compressive strains were analysed separately for each intervertebral disc. The distribution of data of each parameter was tested for normality with the Shapiro-Wilk test. All the data are reported as median.

Differences between the left and the right lateral bending were assessed with the Paired *t*-test in case of normality, or with the Wilcoxon matched pairs signed rank test. As there were no significant differences between right and left lateral bending, the mean between the right and the left values of each parameter was computed and used to evaluate the differences among the decompressive treatments.

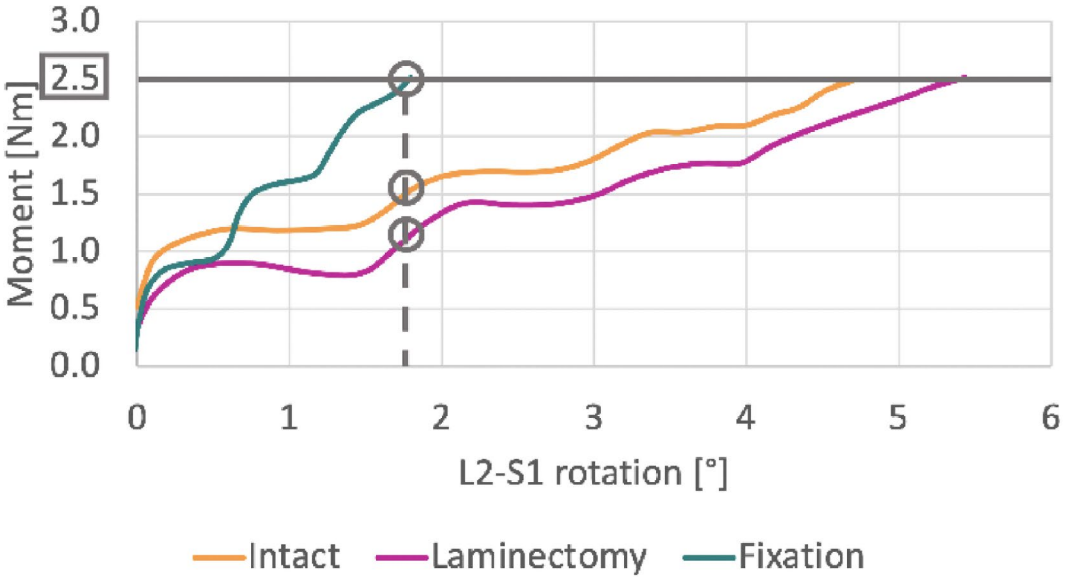

Fig. 5. Plot of the moment versus the L5-S1 rotation for a typical specimen. The range of motion was analysed at the stage where the maximum target moment of 2.5 Nm was reached (grey horizontal line). The strains were measured at the stage where the motion of the L2-S1 spine segment of the intact and laminectomy condition (grey circles) was the same as the fixation reached the 2.5 Nm (grey dashed vertical line).

For the range of motion, the Repeated Measures One-Way ANOVA and the post-hoc Tukey multiple comparison test was performed to assess the effect of the decompressive procedures, in each loading configuration, for the data with a normal distribution. In case of non-normal data, the Friedman test and the post-hoc Dunn's multiple comparison test was used instead.

As the strain data were mostly normal, the effect of the loading configurations, of the conditions and of the interaction between these two factors were assessed for both the tensile and compressive strain for each intervertebral discs (L2-L3, L3-L4, L4-L5 and L5-S1) by means a Repeated Measures Two-Way ANOVA (or a mixed-effects models in case of a missing value) and the post-hoc Tukey's multiple comparison test, with a single pooled variance.

All statistical analyses were performed using GraphPad Prism (Window version 9.3.1, GraphPad Software, La Jolla, CA, USA). Statistical significance was defined as a p-value smaller than 0.05.

Results

DIC correlations were successfully performed for all the conditions, all the loading configurations, and all specimens. Due to a data loss, in the first six specimens the tensile and compressive strain on the intervertebral discs could not be retrieved for the intact condition.

All the data have been averaged among the last three repetitions for each condition and loading configuration (Fig. 3), and then normalized with respect to the intact condition. As no statistically significant differences were found between left and right lateral bending neither for ROM, nor for strains ($p > 0.05$ for all), the mean between left and right bending is reported as "lateral bending".

Errors and repeatability analysis

The zero-strain analysis performed on unloaded images of each loading configuration and condition for each specimen reported a systematic error smaller than 10×10^{-6}, and a random error smaller than 200×10^{-6} in the strain measurements. The intra-specimen repeatability analysis showed that the coefficient of variation among repetitions on the same specimen was 1.3% (average of all specimens) in flexion, 10.4% in extension, 4.4% lateral bending, for the range of motion. For both the tensile and compressive strains, the intra-specimen repeatability analysis focused on mean measured strain value on the intervertebral discs surface. The coefficient of variation among repetitions was 8.4% (average among all specimens and between the tensile and compressive strain) in flexion, 12.2% in extension, 9.4% in lateral bending.

Range of motion

To compare the spine mobility in the different conditions of the spine segment, the motions at full load (2.5 Nm) were compared. After the laminectomy, a clear increase was visible for the range of motion for all the loading configurations (Fig. 6). Laminectomy significantly increased the range of motion by 22% in flexion ($p = 0.028$, post hoc Tukey multiple comparison test) and by 18% in lateral bending ($p = 0.035$) with respect to the intact condition. The slight increase in extension was not significant ($p > 0.999$, post hoc Dunn's multiple comparison test). After the posterior fixation, the ROM decreased in all the loading configurations with respect to the intact condition: the decrease by 69% in extension was significant ($p = 0.013$, post hoc Dunn's multiple

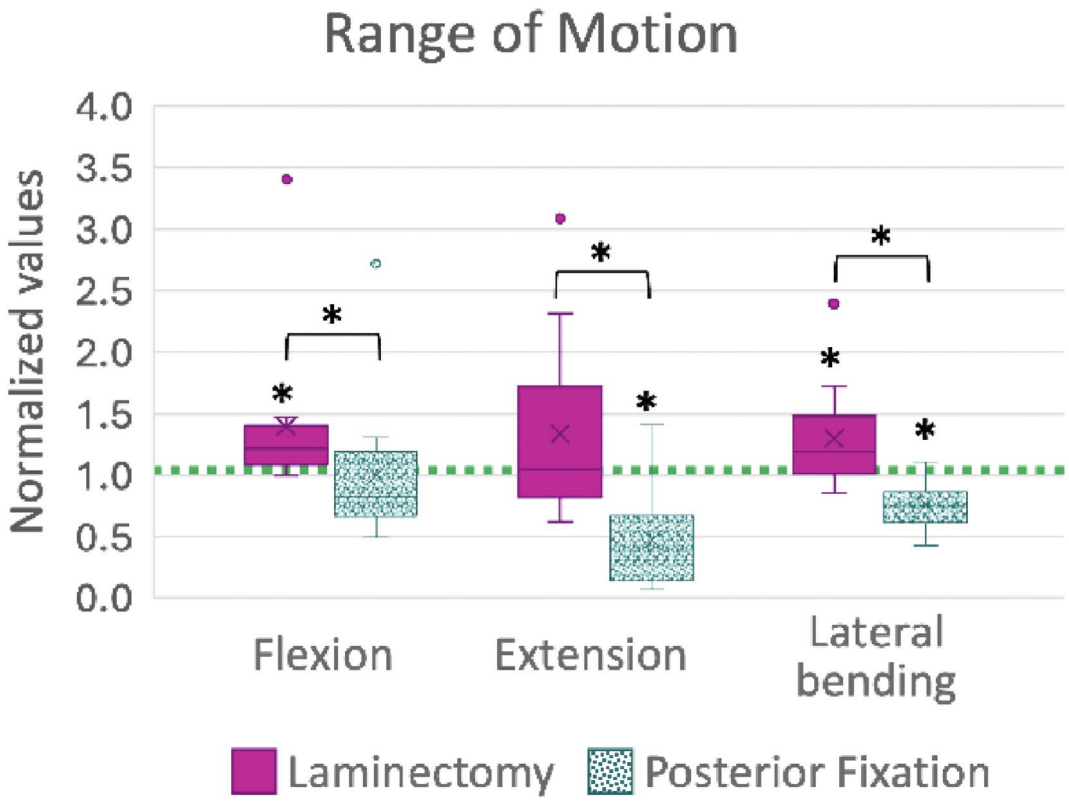

Fig. 6. Range of motion (ROM) in flexion, extension, lateral bending after the two-level laminectomy and posterior fixation. All the data were normalized with respect to the intact condition (dashed green line), and averaged between all the specimens. A value larger than 1.0 indicates an increase of the range of motion with respect to the intact condition. The box plot summarizes the distribution of all 12 specimens tested. The bottom of the box represents the first quartile (25th percentile) of the data; the horizontal line inside the box represents the median of the data, and the top of the box represents the third quartile (75th percentile). The "X" cross represents the mean of the data. The top and bottom whiskers include the maximum and the minimum data, excluding the outliers which are shown as dots. The asterisks * above the box indicate a statistically significant differences with respect to the intact condition ($p < 0.05$). The asterisks * above the squared brackets indicate a significant difference between the laminectomy and fixation conditions.

comparison test), and by 25% in lateral bending was significant ($p = 019$, post hoc Tukey multiple comparison test). A statistically significant decrease of the ROM for all the loading configurations was observed between the laminectomy and the posterior fixation (flexion: $p = 0.002$, lateral bending: $p < 0.001$, post hoc Tukey multiple comparison test; extension: $p = 0.003$, post hoc Dunn's multiple comparison test).

Qualitative analysis of the strain distribution on the surface of the intervertebral discs

To compare the strain in the discs under comparable flexion/extension/bending, the strain maps of the intact and laminectomy conditions of each specimen were analysed at the stage where the motion of the L2-S1 segment was the same as the motion at full load (2.5 Nm) of the same specimen after fixation. Thus, the strains were compared when the spine segments rotated by the same angle (rather than comparing a condition where the same moment was applied, but the spine rotations were not comparable).

In flexion, both the most strained areas (both tensile ε1, and compressive strains ε2) were localized at the mid-height of the each of the discs (Fig. 7). In all the intervertebral discs, the tensile strains were aligned circumferentially in the intact, laminectomy and fixation conditions. Conversely, the compressive strains were aligned axially in all the conditions. In all the intervertebral discs, the area of the discs affected by the highest strains showed the tendency to enlarge from the intact to the posterior fixation condition.

In extension (Fig. 8), the highest tensile strains were localized at the mid-height of all intervertebral discs. The tensile strains were aligned axially, while the compressive strains were mainly aligned circumferentially. The highest compressive strains were mainly located at the interfaces between the bone and the disc. Similar to flexion, the highest tensile strains increased from the intact to the laminectomy condition, and decreased after the posterior fixation, in the two fixed intervertebral discs (L4-L5 and L5-S1). Similar to flexion, the region affected by the highest strains expanded from the intact to the fixation condition in the L2-L3 and L3-L4 discs, which are cranial to the laminectomy and fixation.

The strain distributions for left and lateral bending are reported (Figs. 9 and 10), showing that the effect of the opposite directions of loading was rather specular. In both left and right lateral bending, the highest

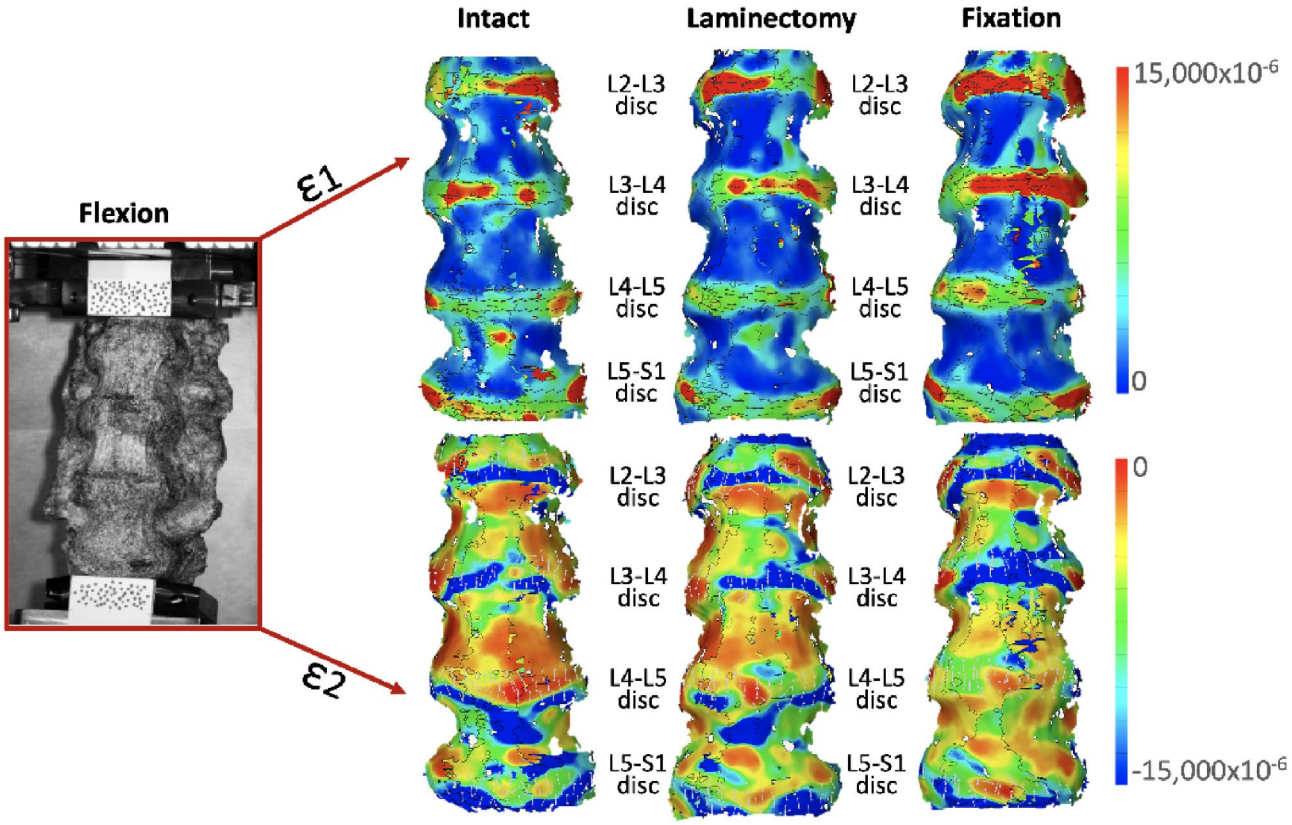

Fig. 7. Flexion: distribution of the maximum (tensile, ε1, top) and minimum (compressive, ε2, bottom) strains on the anterior and lateral surface of a typical specimen. The picture inside the red square on the far left shows the specimens as viewed by the DIC cameras. The strain maps in the intact condition, after laminectomy, and after posterior fixation are reported. The false-colour maps indicate the magnitude of the measured strains (legend on the far right). Some strain peaks are also visible on the anterior longitudinal ligament in front of some of the vertebrae, but these were not relevant for this study. The alignment of the principal strains is shown by the black tensile arrows (ε1) and by the white ones (ε2). Figure published on Figshare (https://doi.org/10.6084/m9.figshare.25823899).

tensile strains were located at mid-height of all intervertebral discs with a circumferential alignment in the lateral side, where the bending was performed. On the opposite side, high tensile strain aligned axially were visible at the interfaces between the bone and the disc. Conversely, the highest compressive strains were located at the interfaces between the bone and the disc and axially aligned, in the lateral part, towards the side where the bending was performed. Similar to the other loading configurations, on the L4-L5 and L5-S1 intervertebral discs, the area affected by the highest strain increased from the intact to laminectomy condition, and decreased after the posterior fixation. The area affected by the highest tensile and compressive strains expanded from the intact to the fixation condition, in the L2-L3 and L3-L4 intervertebral discs (cranial to the treated levels).

The strain maps of the other specimens are displayed in the Supplementary Information, Fig. S2.

Quantitative analysis of the strains on the surface of the intervertebral discs

The statistical analysis of the mean strains on the intervertebral discs provided a clear trend and showed significant variations. The analysis of the largest strains on each disc yielded provided similar trends to the analysis of the mean values, but fewer effects were detected as statistically significant. For this reason, the presentation of the results below will focus on the analysis of the mean values on each disc (Fig. 11; Table 2). The analysis of the largest values is reported in the Supplementary Information, Fig. S3.

Focusing on L4-L5 intervertebral disc (between the two laminectomy levels), both the loading configurations and the spine conditions showed a significant effect for both the tensile and compressive strain (tensile strain: $p < 0.001$ for loading configurations, $p = 0.021$ for spine conditions; compressive strain: $p > 0.001$ for loading configuration, $p = 0.004$ for spine conditions, mixed-effects model). The interaction between the two factors was significant only for the compressive strain ($p = 0.003$, mixed-effects model). The mean tensile strain significantly decreased in flexion after the posterior fixation with respect to the intact spine condition ($p = 0.006$, Tukey's multiple comparison test). A significant decrease of the mean tensile strain was observed also between laminectomy and fixation in extension ($p = 0.045$, Tukey's multiple comparison test). The mean compressive strain decreased in flexion after the posterior fixation with respect to both the intact spine condition and laminectomy ($p < 0.0001$ both, Tukey's multiple comparison test).

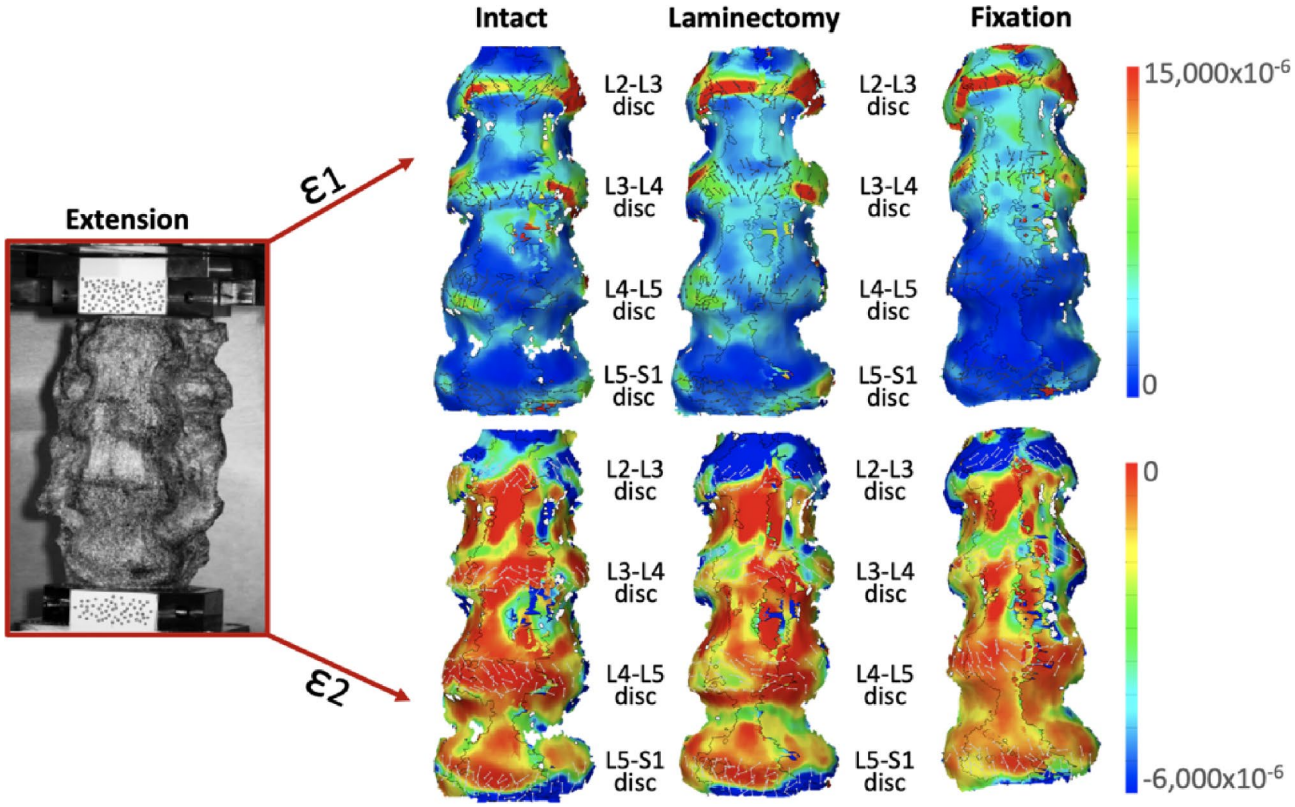

Fig. 8. Extension: distribution of the maximum (tensile, ε1, top) and minimum (compressive, ε2, bottom) strains on the anterior and lateral surface of a typical specimen. The picture inside the red square on the far left shows the specimens as viewed by the DIC cameras. The strain maps in the intact condition, after laminectomy, and after posterior fixation are reported. The false-colour maps indicate the magnitude of the measured strains (legend on the far right). Some strain peaks are also visible on the anterior longitudinal ligament in front of some of the vertebrae, but these were not relevant for this study. The alignment of the principal strains is shown by the black tensile arrows (ε1) and by the white ones (ε2). Figure published on Figshare (https://doi.org/10.6084/m9.figshare.25823905).

Focusing on the L5-S1 intervertebral disc, which was caudal to the decompressive surgery and was included in the posterior fixation, the loading configurations significantly impacted both the tensile and compressive strain (tensile strain: $p < 0.001$; compressive: $p < 0.0001$, mixed-effects model). The spine conditions showed a significant effect only for the tensile strain ($p = 0.046$, mixed-effects model). The interaction between the two factors was not significant neither for the tensile nor for the compressive strain. Both the mean tensile and compressive strain showed a significant decrease after the posterior fixation with respect to the intact spine condition in flexion (tensile strain: $p = 0.021$; compressive strain: $p = 0.007$, Tukey's multiple comparison test). The mean compressive strain significant decrease after the fixation also compared to the laminectomy ($p = 0.021$, Tukey's multiple comparison test).

Focusing on the disc cranial to both the decompressive treatment and the fixation (L3-L4), the loading configurations showed a significant effect on both the tensile and compressive strains (tensile strain: $p = 0.003$; compressive: $p = 0.002$, mixed-effects model). The spine condition significantly impacted the tensile strain ($p = 0.020$, mixed-effects model). Conversely, the interaction between the two factors was not significant, neither for the tensile nor for the compressive strain (tensile strain: $p = 0.28$; compressive: $p = 0.12$, mixed-effects model). The tensile strain significantly increased after the posterior fixation compared to the laminectomy in flexion and lateral bending (flexion: $p = 0.018$; lateral bending: $p = 0.041$, Tukey's multiple comparison test). After the posterior fixation, also the compressive strain significantly increased with respect to both the intact spine condition and the laminectomy ($p = 0.012$ and $p = 0.021$, Tukey's multiple comparison test).

Focusing on the L2-L3 intervertebral disc, two levels above the decompressive treatment and fixation, the loading configurations showed a significant effect in the compressive strain ($p = 0.031$, mixed-effects model). The tensile strain significantly increased in lateral bending after the posterior fixation with respect to both the intact spine condition and the laminectomy ($p = 0.036$ and $p = 0.022$, Tukey's multiple comparison test). No other significant effect was observed on this disc.

The data plotted here are reported in table format in the Supplementary Information, Table S2.

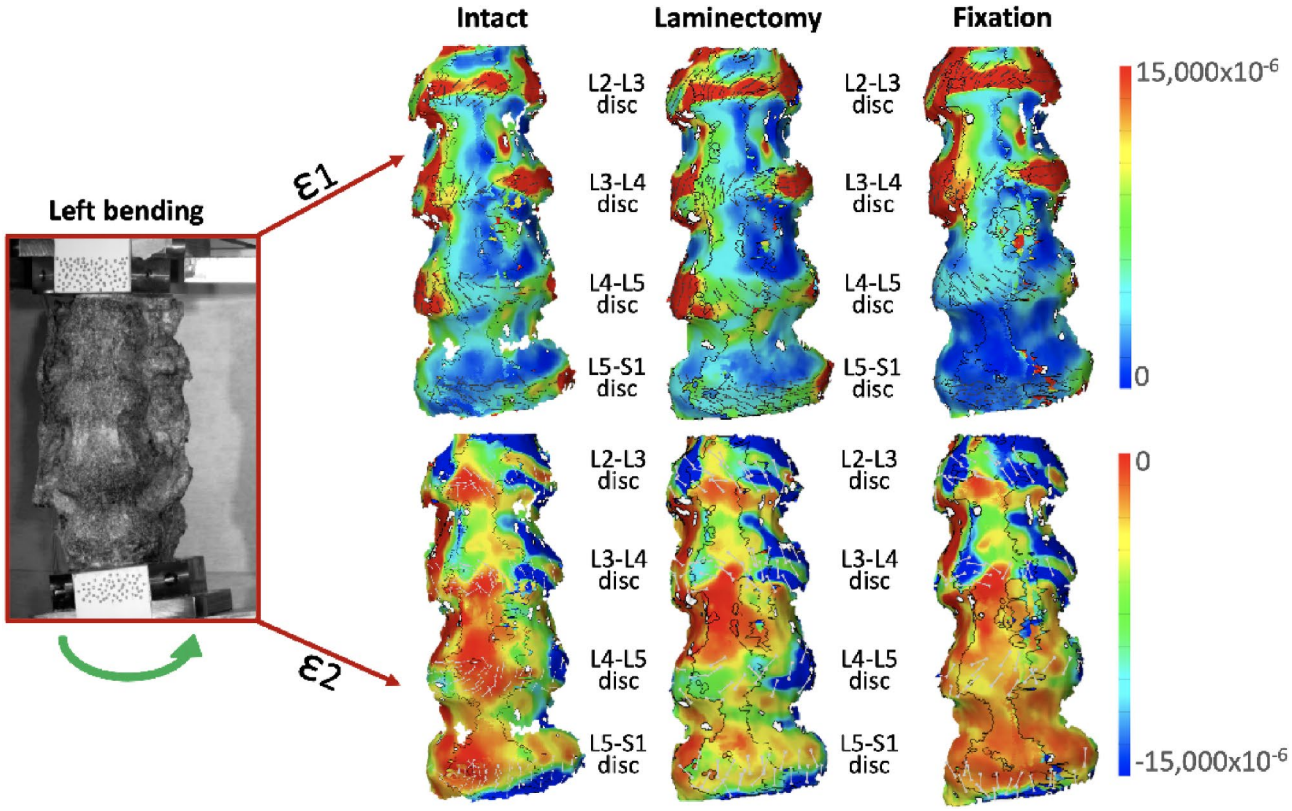

Fig. 9. Left lateral bending: distribution of the maximum (tensile, ε1, top) and minimum (compressive, ε2, bottom) strains on the anterior and lateral surface of a typical specimen. The picture inside the red square on the far left shows the specimens as viewed by the DIC cameras. The strain maps in the intact condition, after laminectomy, and after posterior fixation are reported. The false-colour maps indicate the magnitude of the measured strains (legend on the far right). Some strain peaks are also visible on the anterior longitudinal ligament in front of some of the vertebrae, but these were not relevant for this study. The alignment of the principal strains is shown by the black tensile arrows (ε1) and by the white ones (ε2). Figure published on Figshare (https://doi.org/10.6084/m9.figshare.25823911).

Discussion

This study aimed to assess how the mobility of the lumbar spine is affected by a two-level laminectomy and the posterior fixation, in case of decompressive treatments, and whether these techniques impact the strain distribution of the intervertebral discs, between the treated levels or in the adjacent levels. Twelve L2-S1 human spine segment were tested in flexion, extension, and lateral bending before and after the simulation of the different decompressive treatments. The changes of the biomechanics of the lumbar spine were measured by means of the Digital Image Correlation.

Both the systematic and random errors on the DIC- measured strains were acceptable[32] with respect to the range of strains actually measured, and in accordance with similar previous DIC analysis[29,33].The coefficient of variation between repetitions was less than 12.5% for all the specimens in each loading configuration, confirming that the entire test method had a good repeatability.

As expected, laminectomy significantly increased the mobility of the lumbar spine in flexion and lateral bending with respect to the intact spine. Removal of posterior arch, including the supraspinous and interspinous ligaments, in addition to the ligamentum flavum, allowed to increase the range of motion of the spine segments. Conversely, in extension, the presence of the facet joint, which in a healthy condition naturally constrain the posterior movement of the spine, limited the excursion of the lumbar spine also after the laminectomy, with no significant increase of the range of motion. Posterior fixation significantly decreased the ROM in extension and lateral bending if compared to the intact condition, similar to previous literature[34]. Conversely, fixation did not significantly impact the range of motion in flexion. Posterior fixation is intended to recover the natural alignment of the spine. In this study, the L4-S1 posterior fixation aimed to restore the lumbar lordosis of the distal lumbar spine after the two-level laminectomy. The lumbar lordosis is not homogenously distributed across the different lumbar levels: the L4-S1 segment is overall responsible for 62% of lordosis, whereas the L1-L4 segment accounts for 38% of lordosis[35]. Similarly, the intervertebral ROM of each lumbar spine level is strictly related within the position along the spine[36]. Indeed, Galbusera et al., 2021[36] reported that the ROM at both the L4-L5 and L5-S1 levels is higher compared to the ROM of the other levels within the lumbar spine. Our findings outlined, thus, that fixing and reducing the possible excursion of the L4-S1 segment is reflected by an increase in the ROM of cranial part of the lumbar spine, so that the entire ROM of segment could retain the same mobility in flexion.

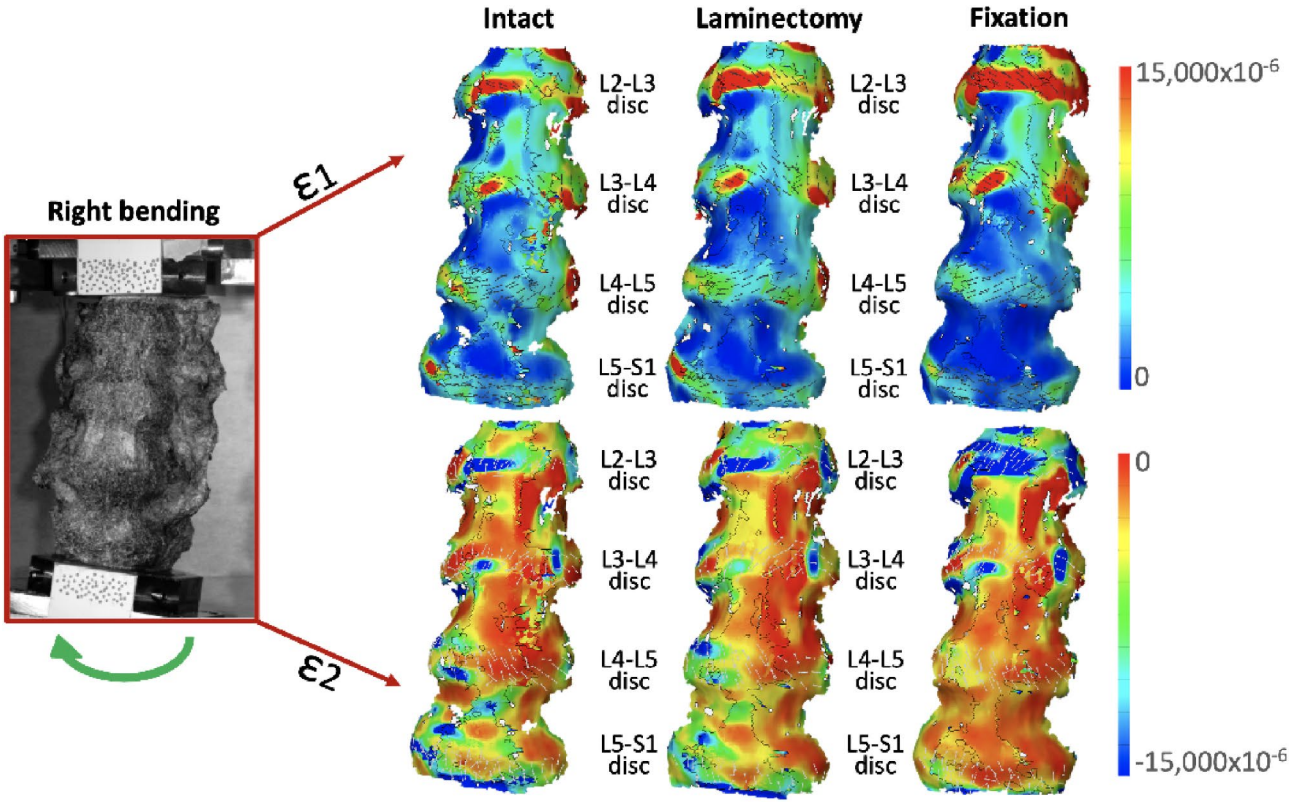

Fig. 10. Right lateral bending: distribution of the maximum (tensile, ε1, top) and minimum (compressive, ε2, bottom) strains on the anterior and lateral surface of a typical specimen. The picture inside the red square on the far left shows the specimens as viewed by the DIC cameras. The strain maps in the intact condition, after laminectomy, and after posterior fixation are reported. The false-colour maps indicate the magnitude of the measured strains (legend on the far right). Some strain peaks are also visible on the anterior longitudinal ligament in front of some of the vertebrae, but these were not relevant for this study. The alignment of the principal strains is shown by the black tensile arrows (ε1) and by the white ones (ε2). Figure published on Figshare (https://doi.org/10.6084/m9.figshare.25823914).

Conversely, the fixation of the distal lumbar spine reduced the ROM of the entire lumbar spine in extension and lateral bending. As a result of the increase in ROM after laminectomy and of the decrease after posterior fixation both with respect to the intact condition, the posterior fixation decreased the ROM with respect to the laminectomy condition in all the loading configurations.

Results similar to what this study found were reported in the literature, although for a single-level laminectomy and fixation: a significant ROM increase after the laminectomy[37,38], and a significant decrease after the posterior fixation were found[39,40]. Also Delank et al., 2010[41] reported a ROM reduction after posterior fixation, by applying a moment of 3.5 Nm, which is closer to the load applied in the present study. Bisschop et al., 2015[19] reported a significant increase in the segmental ROM at the treated level after one-level laminectomy and a significant decrease after one-level posterior fixation in flexion-extension and lateral bending, while they reported that the ROM in the level adjacent to the fixation decreased in lateral bending (but not in flexion-extension).

In addition, comparable variations of ROM between the intact and laminectomy conditions were found between this study and the work of Burkhard et al., 2023[39], . Conversely, it is not possible to compare the effect of posterior fixation with Burkhard et al., because of the different length of the specimens used: while in the present studya L2-S1 segment was tested, Burkhard et al. tested functional spinal units.

To assess the alterations of the strain distribution in the intervertebral discs due to laminectomy and fixation, both tensile and compressive strains were compared keeping the same L2-S1 spine segment rotation after posterior fixation as a reference.

Focusing on the L4-L5 intervertebral disc (which was included in the posterior fixation), as expected a clear decrease of the strains (both tensile and compressive) after posterior fixation in all the loading configurations was found: the explanation is that most of the load is transferred along the posterior rods, instead of the intervertebral disc. Conversely, comparing the same rotation, laminectomy increased the area affected by higher values of strain, but did not induce abnormal strain concentration, which could be a risk for the integrity of the disc.

Similar to L4-L5, also for the L5-S1 intervertebral disc (which was included in the posterior fixation), both the tensile and compressive strains decreased after fixation, with a significant effect especially in flexion. The

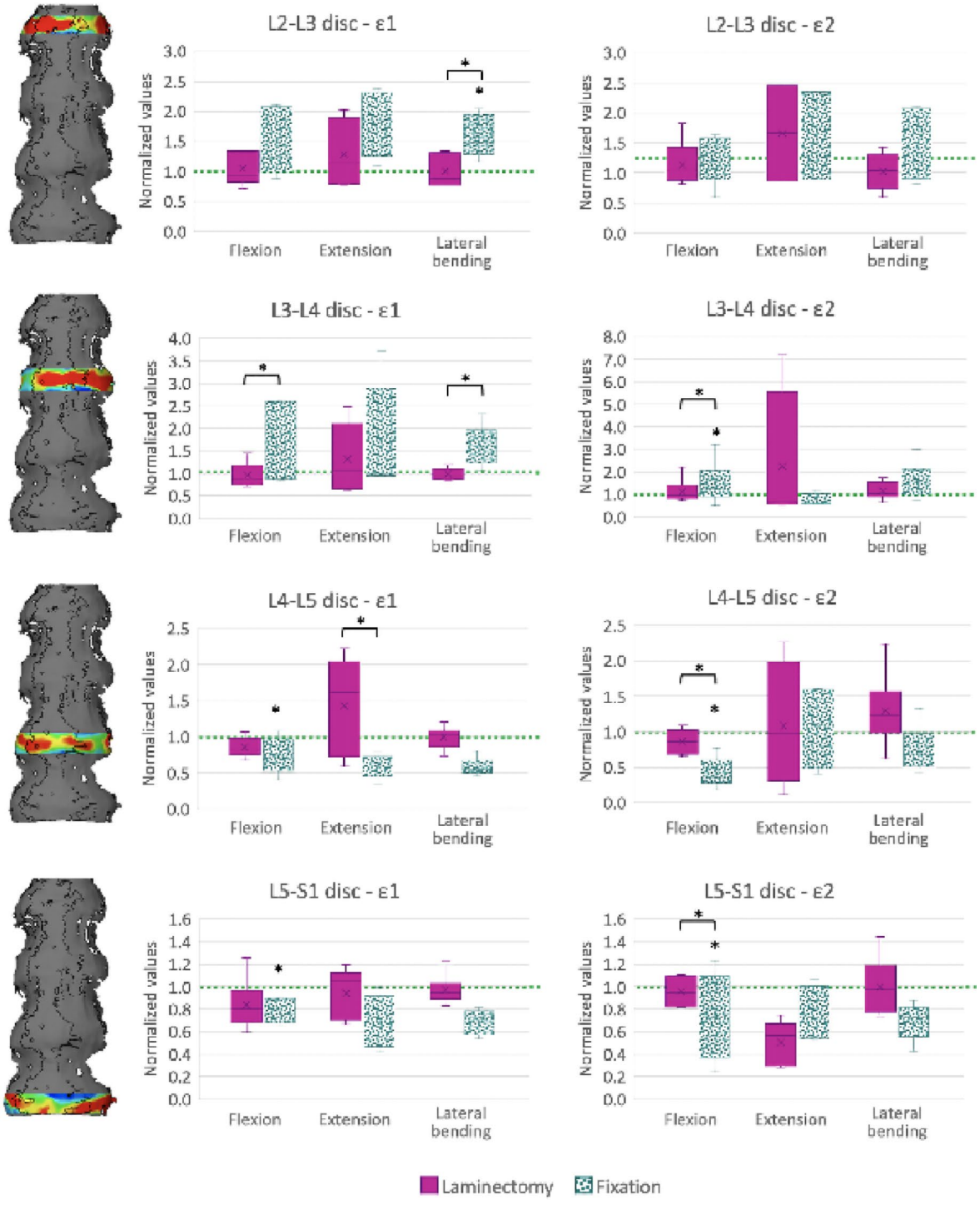

Fig. 11. Mean tensile (ε1, left plots) and compressive (ε2, right plots) strains on the L2-L3, L3-L4, L4-L5 and L5-S1 intervertebral discs, in flexion, extension, and lateral bending after the two-level laminectomy, and after posterior fixation. All the data were normalized with respect to the intact condition (dashed green line), and averaged between all the specimens. A value larger than 1.0 indicates an increase of strain magnitude with respect to the intact condition. As data for the intact condition were lost for the first six specimens, the box plot summarizes the distribution of the remaining six specimens. The bottom of the box represents the first quartile (25th percentile) of the data; the horizontal line inside the box represents the median of the data and the top of the box represents the third quartile (75th percentile). The "X" cross represents the mean of the data. The top and bottom whiskers include the maximum and the minimum data, excluding the outliers which are shown as dots. The asterisks * above the box indicate a statistically significant differences (post-hoc) with respect to the intact condition ($p < 0.05$). The asterisks * above the squared brackets indicate a significant difference between the laminectomy and fixation conditions. The results of the Repeated Measures Two-Way ANOVA are reported in Table 2.

	L2-L3		L3-L4		L4-L5		L5-S1	
	ε1	ε2	ε1	ε2	ε1	ε2	ε1	ε2
Loading configurations	0.057	0.031*	0.003*	0.002*	< 0.001*	< 0.001*	< 0.001*	< 0.0001*
Spine conditions	0.065	0.205	0.020*	0.237	0.021*	0.004*	0.047*	0.109
Interaction between factors	0.316	0.792	0.277	0.122	0.202	0.003*	0.564	0.117

Table 2. Results of the repeated measures two-way ANOVA (P-values) on the mean values of both tensile (ε1) and compressive (ε2) strain on each intervertebral disc. The factor 'Loading configurations' is referred to flexion, extension, and lateral bending. The factor 'Spine conditions' is referred to intact, laminectomy and posterior fixation. As data for the intact condition were lost for the first 6 specimens, the statistical analysis was based on the remaining six specimens. A p-value < 0.05 was considered statistically significant (*).

laminectomy did not impact this strain at this level, confirming that the anterior and lateral part of the spine, together with the preservation of the facet joint[22], can still compensate for the absence of the posterior arches.

On the L3-L4 intervertebral disc (which was cranial to both the laminectomy and posterior fixation), flexion resulted as a critical configuration significantly increasing both the tensile and compressive strain after posterior fixation. Moreover, the tensile strains increased after posterior fixation also in lateral bending. Due to the anatomy of the disc, the stretching of the lateral fibres seemed one of the most challenging configurations for the intervertebral disc. This abnormal increase of the strain could be one of the clinical causes of the development of adjacent segment degeneration.

On the L2-L3 intervertebral disc (which was two levels cranial to the treated levels), a similar trend to the L3-L4 disc could be observed, but only lateral bending resulted as a challenging configuration, with remarkably high tensile strains after the posterior fixation.

Some finite elements (FE) studies focused on analyzing the biomechanical effect of laminectomy and posterior fixation in the lumbar spine. Some of these studies investigated the effect of the bone resection during laminectomy reporting that larger amount of bone resection leads to greater biomechanical changes and increases the risk of iatrogenic instability[42,43]. This finding is in agreement with the findings of the present study, where laminectomy increased the range of motion significantly more than hemilaminectomy. Chen et al., 2005[44], reported a significant increase on the strain in the above disc adjacent to the disc where the laminectomy was simulated, in flexion. These results are not in agreement with the results from the present experiments, possibly in relation to the large moment applied to their FE model (10Nm).

This study has some limitations that must be discussed. Due to the loss of some data for the intact condition, some analyses have been performed without the inclusion of such specimens. Unfortunately, it was not possible to repeat the tests because laminectomy had been already performed on these specimens. In the worst case, at least six specimens have been included, which is a number of specimens sufficient to perform a statistical analysis and which is used in other studies in the literature[18,23,40]. Another limitation of this study is the use of segments of spine obtained by cadavers. Similar to most of the other cadaver studies, the effect of muscular forces, of the whole spine itself and of the sagittal balance on the spine could not be included. However, this study compared each specimen to itself in the intact state, after the laminectomy and after the posterior fixation: as changes with respect to the respective intact were quantified, the biomechanical impact of these treatments could be successfully assessed. The relatively low moment applied during the mechanical tests was another limitation of this study. A moment of 2.5 Nm was intentionally applied in order to avoid damaging the specimens during all the different repetitions in each loading configuration, also considering that the spine segments were expected to become more unstable after laminectomy. The magnitude of the moment applied in this study was at the bottom of the range that can be found in the literature[23]. It is possible that higher moments could alter the strain distribution on the intervertebral discs with a different trend. However, the changes on the range of motion found in this study were comparable to those reported in the literature as a consequence of the application of similar and larger moments. In addition, it was not possible to include magnetic resonance scans of the intervertebral discs in the study. This would have provided relevant information on the status of the intervertebral discs. In fact, the condition of the nucleus pulposus and the annulus fibrosus could influence the biomechanical behaviour of the lumbar spine.

Conclusion

In conclusion, this ex vivo study investigated the impact of the two-level laminectomy and L4-S1 posterior fixation on the biomechanics of the lumbar spine, in terms of range of motion of the entire lumbar segment, and of the strain distribution on the intervertebral discs. This study confirmed that laminectomy increases the mobility of the lumbar spine in flexion and lateral bending, and that fixation reduces the range of motion the lumbar spine in all the loading configurations.

In addition, this study for the first time showed that flexion is one the most critical loading configuration after the posterior fixation in the most cranial adjacent disc (L3-L4), as it increased both the tensile and compressive strains in the disc itself. Lateral bending is also a challenging loading configuration dramatically increasing the tensile strains in the adjacent disc. These results could elucidate the mechanisms underlying the high incidence of adjacent segment degeneration after posterior fixation.

Data availability

All data analysed during this study are included in this published article (and its Supplementary Information Files). The raw data used are available from the corresponding author upon request.

Received: 31 May 2024; Accepted: 21 November 2024
Published online: 03 December 2024

References

1. Arbit, E. & Pannullo, S. Lumbar stenosis: a clinical review. *Clin. Orthop. Relat. Res.* **384**, 137–143 (2001).
2. Smith, Z. A. et al. Biomechanical effects of a unilateral approach to minimally invasive lumbar decompression. *PLoS One*. **9**, e92611 (2014).
3. Issack, P. S., Cunningham, M. E., Pumberger, M., Hughes, A. P. & Cammisa, F. P. Degenerative lumbar spinal stenosis: evaluation and management. *J. Am. Acad. Orthop. Surg.* **20**, 527–535 (2012).
4. Abbas, J. et al. Socioeconomic and physical characteristics of individuals with degenerative lumbar spinal stenosis. *Spine*. **38**, E554–561 (2013).
5. Deyo, R. A., Gray, D. T., Kreuter, W., Mirza, S. & Martin, B. I. United States trends in lumbar fusion surgery for degenerative conditions. *Spine*. **30**, 1441–1445 (2005).
6. Caputy, A. J. & Luessenhop, A. J. Long-term evaluation of decompressive surgery for degenerative lumbar stenosis. *J. Neurosurg.* **77**, 669–676 (1992).
7. Ganz, J. C. Lumbar spinal stenosis: postoperative results in terms of preoperative posture-related pain. *J. Neurosurg.* **72**, 71–74 (1990).
8. Ramhmdani, S. et al. Iatrogenic spondylolisthesis following open lumbar laminectomy: Case Series and Review of the literature. *World Neurosurg.* **113**, e383–e390 (2018).
9. Adogwa, O. et al. Cost per quality-adjusted life year gained of revision fusion for lumbar pseudoarthrosis: defining the value of surgery. *J. Spinal Disord. Tech.* **28**, 101–105 (2015).
10. Deyo, R. A. et al. Revision surgery following operations for lumbar stenosis. *J. Bone Joint Surg. Am.* **93**, 1979–1986 (2011).
11. Försth et al. A Randomized, Controlled Trial of Fusion surgery for lumbar spinal stenosis. *N. Engl. J. Med.* **374**, 1413–1423 (2016).
12. Austevoll, I. M. et al. Decompression with or without Fusion in degenerative lumbar spondylolisthesis. *N Engl. J. Med.* **385**, 526–538 (2021).
13. Ulrich, N. H. et al. Incidence of revision surgery after decompression with vs without Fusion among patients with degenerative lumbar spinal stenosis. *JAMA Netw. Open.* **5**, e2223803 (2022).
14. Ekman, P., Möller, H. & Hedlund, R. The long-term effect of posterolateral fusion in adult isthmic spondylolisthesis: a randomized controlled study. *Spine J.* **5**, 36–44 (2005).
15. Berjano, P., Damilano, M., Pejrona, M., Langella, F. & Lamartina, C. Revision surgery in distal junctional kyphosis. *Eur. Spine J.* **29**, 86–102 (2020).
16. Aota, Y., Kumano, K. & Hirabayashi, S. Postfusion instability at the adjacent segments after rigid pedicle screw fixation for degenerative lumbar spinal disorders. *J. Spinal Disord.* **8**, 464–473 (1995).
17. Montanari, S. et al. Correlation between Sagittal Balance and mechanical distal junctional failure in Degenerative Pathology of the spine: a retrospective analysis. *Global Spine J.* https://doi.org/10.1177/21925682231195954 (2023).
18. Ma, J. et al. Evaluation of the stress distribution change at the adjacent facet joints after lumbar fusion surgery: a biomechanical study. *Proc. Inst. Mech. Eng. H.* **228**, 665–673 (2014).
19. Bisschop, A. et al. The effects of single-level instrumented lumbar laminectomy on adjacent spinal biomechanics. *Global Spine J.* **5**, 39–48 (2015).
20. Shenkin, H. A. & Hash, C. J. Spondylolisthesis after multiple bilateral laminectomies and facetectomies for lumbar spondylosis. Follow-up review. *J. Neurosurg.* **50**, 45–47 (1979).
21. Fox, M. W., Onofrio, B. M., Onofrio, B. M. & Hanssen, A. D. Clinical outcomes and radiological instability following decompressive lumbar laminectomy for degenerative spinal stenosis: a comparison of patients undergoing concomitant arthrodesis versus decompression alone. *J. Neurosurg.* **85**, 793–802 (1996).
22. Widmer, J. et al. Biomechanical contribution of spinal structures to stability of the lumbar spine-novel biomechanical insights. *Spine J.* **20**, 1705–1716 (2020).
23. Wilke, H. J., Wenger, K. & Claes, L. Testing criteria for spinal implants: recommendations for the standardization of in vitro stability testing of spinal implants. *Eur. Spine J.* **7**, 148–154 (1998).
24. Danesi, V., Zani, L., Scheele, A., Berra, F. & Cristofolini, L. Reproducible reference frame for in vitro testing of the human vertebrae. *J. Biomech.* **47**, 313–318 (2014).
25. Techens, C. et al. Biomechanical consequences of cement discoplasty: an in vitro study on thoraco-lumbar human spines. *Front. Bioeng. Biotechnol.* **10**, 1040695 (2022).
26. Cottrell, J. M., van der Meulen, M. C. H., Lane, J. M. & Myers, E. R. Assessing the stiffness of spinal fusion in animal models. *HSS J.* **2**, 12–18 (2006).
27. Palanca, M., Brugo, T. M., Cristofolini, L., USE OF DIGITAL & IMAGE CORRELATION TO INVESTIGATE THE BIOMECHANICS OF THE VERTEBRA. *J. Mech. Med. Biol.* **15**, 1540004 (2015).
28. Cristofolini, L. Overview of digital image correlation. in Experimental Stress Analysis for Materials and Structures: Stress Analysis Models for Developing Design Methodologies (eds Freddi, A., Olmi, G. & Cristofolini, L.). Springer International Publishing, 187–213. https://doi.org/10.1007/978-3-319-06086-6_5. (2015).
29. Palanca, M., Marco, M., Ruspi, M. L. & Cristofolini, L. Full-field strain distribution in multi-vertebra spine segments: an in vitro application of digital image correlation. *Med. Eng. Phys.* **52**, 76–83 (2018).
30. Lionello, G., Sirieix, C. & Baleani, M. An effective procedure to create a speckle pattern on biological soft tissue for digital image correlation measurements. *J. Mech. Behav. Biomed. Mater.* **39**, 1–8 (2014).
31. Montanari, S. et al. Effect of two-level decompressive procedures on the biomechanics of the lumbo-sacral spine: an ex vivo study. *Front. Bioeng. Biotechnol.* **12**, 1400508 (2024).
32. Palanca, M., Tozzi, G. & Cristofolini, L. The use of digital image correlation in the biomechanical area: a review. *Int. Biomech.* **3**, 1–21 (2016).
33. Palanca, M. et al. The strain distribution in the lumbar anterior longitudinal ligament is affected by the loading condition and bony features: an in vitro full-field analysis. *PLoS ONE.* **15**, e0227210 (2020).
34. La Barbera, L. et al. Load-sharing biomechanics of lumbar fixation and fusion with pedicle subtraction osteotomy. *Sci. Rep.* **11**, 3595 (2021).
35. Pesenti, S. et al. The amount of proximal lumbar lordosis is related to pelvic incidence. *Clin. Orthop. Relat. Res.* **476**, 1603 (2018).
36. Galbusera, F. et al. ISSLS Prize in Bioengineering Science 2021: in vivo sagittal motion of the lumbar spine in low back pain patients-a radiological big data study. *Eur. Spine J.* **30**, 1108–1116 (2021).
37. Bisschop, A. et al. Single level lumbar laminectomy alters segmental biomechanical behavior without affecting adjacent segments. *Clin. Biomech. (Bristol Avon).* **29**, 912–917 (2014).

38. Lener, S. et al. The effect of various options for decompression of degenerated lumbar spine motion segments on the range of motion: a biomechanical in vitro study. *Eur. Spine J.* **32**, 1358–1366 (2023).
39. Burkhard, M. D. et al. Biomechanics after spinal decompression and posterior instrumentation. *Eur. Spine J.* **32**, 1876–1886 (2023).
40. Costa, F. et al. Bone-preserving decompression procedures have a minor effect on the flexibility of the lumbar spine. *J. Korean Neurosurg. Soc.* **61**, 680–688 (2018).
41. Delank, K. S. et al. How does spinal canal decompression and dorsal stabilization affect segmental mobility? A biomechanical study. *Arch. Orthop. Trauma. Surg.* **130**, 285–292 (2010).
42. Zander, T., Rohlmann, A., Klöckner, C. & Bergmann, G. Influence of graded facetectomy and laminectomy on spinal biomechanics. *Eur. Spine J.* **12**, 427–434 (2003).
43. Spina, N. T., Moreno, G. S., Brodke, D. S., Finley, S. M. & Ellis, B. J. Biomechanical effects of laminectomies in the human lumbar spine: a finite element study. *Spine J.* **21**, 150–159 (2021).
44. Chen, C. S. et al. Biomechanical analysis of the disc adjacent to posterolateral fusion with laminectomy in lumbar spine. *J. Spinal Disord Tech.* **18**, 58–65 (2005).

Acknowledgements

The authors wish to thank Fabio Norvillo, Alberto Bazzocchi and Marco Miceli for the CT scans; Franco Pontòn Pasquale and Paola Valentina Gonzalez Rodriguez for the help with the analysis of the strain data; Cristiana Griffoni for the administrative support and advices; Giulia Galteri for the help during the biomechanical tests; Francesco Vai, Stefano Monti, Roberto Budini and Matteo Vanzi for the technical help in preparing the test set-ups; Matteo Facchini for the preparation of the artwork.

Author contributions

S.M. conducted the experiment, performed all the mechanical tests, acquired and analysed the data and performed the statistical analysis with the supervision of L.C. G.B.B and E.S. performed the decompressive surgery on the specimens. S.M wrote the manuscript text, supplementary information, and prepared the figures. L.C., A.G. and A.C. found the fundings of this research. A.C. administrated the project. L.C., A.C., R.S., A.G. developed the concept of the project whereas L.C. and S.M. concretely designed it. All authors contributed to the refinement of the study protocol, reviewed the manuscript and approved the final version.

Funding

This study was partly funded by Region Emilia Romagna (FIN-RER "Archimede" project, Grant E45J19000810002), and partly founded by the European Union, HEU topic HLTH-2022-12-01: 'METASTRA' project grant 101080135).

Declarations

Competing interests

The authors declare no competing interests.

Additional information

Supplementary Information The online version contains supplementary material available at https://doi.org/10.1038/s41598-024-80741-3.

Correspondence and requests for materials should be addressed to L.C.

Reprints and permissions information is available at www.nature.com/reprints.

Publisher's note Springer Nature remains neutral with regard to jurisdictional claims in published maps and institutional affiliations.